Microbial Cell Factories

https://doi.org/10.1186/s12934-026-02976-1

Article in Press

Transcription factor MtCLR-2 regulates cellulase production via direct modulation of *Mtegl2* and *Mtbgl1* expression in *Myceliophthora thermophila*

Received: 3 December 2025

Accepted: 24 February 2026

Published online: 27 April 2026

Cite this article as: Lai Y., Wang J., Xie N. *et al.* Transcription factor MtCLR-2 regulates cellulase production via direct modulation of *Mtegl2* and *Mtbgl1* expression in *Myceliophthora thermophila*. *Microb Cell Fact* (2026). https://doi.org/10.1186/s12934-026-02976-1

Yapeng Lai, Juan Wang, Ning Xie, Gang Liu & Donnabella C. Lacap-Bugler

Transcription factor MtCLR-2 regulates cellulase production via direct modulation of *Mtegl2* and *Mtbgl1* expression in *Myceliophthora thermophila*

Yapeng Lai[1,2], Juan Wang[1], Ning Xie[1], Gang Liu[1]*, Donnabella C. Lacap-Bugler[2]*

* **Correspondence**

Gang Liu

zjuliug@szu.edu.cn

Donnabella C. Lacap-Bugler

dlacapbu@aut.ac.nz

[1] Shenzhen Key Laboratory of Microbial Genetic Engineering, College of Life Sciences and Oceanography, Shenzhen University, Shenzhen, 518055, China

[2] School of Science, Faculty of Health and Environmental Science, Auckland University of Technology, Auckland, 1010, New Zealand

Transcription factor MtCLR-2 regulates cellulase production via direct modulation of *Mtegl2* and *Mtbgl1* expression in *Myceliophthora thermophila*

Abstract

Background: The thermophilic fungus *Myceliophthora thermophila* can secrete large amounts of lignocellulolytic enzymes, such as cellulases and xylanases, which are regulated by multiple transcription factors. However, the understanding of the regulatory mechanism of cellulase gene expression in *M. thermophila* is limited. Here, we characterized the function of MtCLR-2, a *M. thermophila* ortholog of CLR-2, a key cellulolytic transcriptional regulator initially identified in *Neurospora crassa*.

Results: Deletion of *Mtclr-2* significantly reduced cellulase activities, particularly affecting endoglucanase production, whereas overexpression of *Mtclr-2* led to elevation in cellulase secretion when *M. thermophila* was grown on Avicel. Subcellular localization assay of MtCLR-2 fused to green fluorescent protein (GFP) indicated that MtCLR-2 is localized to the nucleus. Real-time quantitative reverse transcription PCR (RT-qPCR) analysis revealed that disruption of *Mtclr-2* caused a decrease in transcript levels of the β-glucosidase gene *bgl1* (*MYCTH_66804*) and the endoglucanase gene *egl2* (*MYCTH_86753*) throughout the stages of growth in cellulose medium. Furthermore,

electrophoretic mobility shift assays (EMSAs) demonstrated that MtCLR-2 directly binds to the promoter regions of *bgl1* and *egl2* in a zinc-dependent manner. The comparative transcriptomic analysis also showed that MtCLR-2 positively regulates the expression of ribosomal protein genes under cellulosic conditions.

Conclusions: These findings contribute to a better understanding of the regulatory network governing cellulase gene expression and provide a potential target for boosting cellulase biosynthesis in *M. thermophila*.

Keywords *Myceliophthora thermophila*, Cellulase, MtCLR-2, Gene expression, Transcriptomic analysis, Ribosomal protein genes

Background

Lignocellulose, the most abundant renewable energy source on Earth, can be converted into fermentable sugars for the production of biofuels and value-added biochemicals in biorefineries [1]. The primary components of lignocellulosic material are cellulose, hemicellulose, and lignin, with cellulose accounting for the highest proportion (40-50%) [2]. The complete hydrolysis of cellulose requires the concerted activities of three complementary cellulase enzymes, endo-1,4-β-glucanase (EC 3.2.1.4), cellobiohydrolase (EC 3.2.1.91), and β-glucosidase (EC 3.2.1.21). These three cellulases act synergistically to decompose cellulose to release glucose as the final product that can be subsequently fermented into ethanol [3]. In addition, lytic polysaccharide

monooxygenases (LPMOs; AA9) have been shown to work in synergy with cellulolytic enzymes during the decomposition of the recalcitrant cellulose [4]. These copper-dependent enzymes oxidatively cleave glycosidic bonds of the cellulose when reducing agents are present, thus improving the efficiency of cellulases and promoting the enzymatic conversion of cellulose [5].

Filamentous fungi are highly efficient decomposers of lignocellulose in the terrestrial biosphere due to their ability to secrete a broad spectrum and large amounts of extracellular enzymes associated with the deconstruction of plant-derived biomass [6, 7]. Among others, *Myceliophthora thermophila* is known to produce a wide array of thermostable carbohydrate-active enzymes (CAZymes) involved in lignocellulose degradation [8, 9]. Recently, this fungus has been genetically modified to produce cellulases and xylanases, as well as biochemicals and biofuels, such as fumaric acid, malic acid, and ethanol [10-13], based on the current omics technologies and fungal genome editing tools [10, 14]. The *M. thermophila* genome encodes at least eight β-glucosidases (BGLs), seven endoglucanases (EGLs), and seven cellobiohydrolases (CBHs) [15]. Among them, *egl2* (MYCTH_86753), *cbh1* (MYCTH_109566) and *cbh2* (MYCTH_66729), and *bgl1* (MYCTH_66804), which encode endoglucanase, cellobiohydrolases, and β-glucosidase, respectively, exhibit high transcript levels and secretion quantities when grown on various sources of lignocellulosic biomass compared to glucose [8, 16, 17]. These extracellular enzymes thus represent the major cellulases of *M. thermophila*. Therefore, a better understanding of the regulatory mechanism

governing the expression of these cellulase genes would facilitate fungal strain engineering and elevate cellulase production in *M. thermophila*.

The transcriptional induction of cellulases or xylanases is strictly controlled by transcription factors [18, 19]. In *M. thermophila*, a couple of regulators that are involved in the lignocellulose depolymerization were identified, including MtXyr1, MtCre1, MtCLR-4, and MtTRC-1. MtXyr1 not only regulates the expression of genes encoding xylanolytic enzymes but also controls genes associated with pentose transport and catabolism, while having no noticeable effect on cellulase secretion [20, 21]. MtCre1 acts as the primary transcriptional repressor of cellulolytic genes, and its silencing or disruption upregulates the transcription of cellulase genes and enhances cellulase production under inducing conditions [10, 22]. Analogous to its homolog CLR-4 in *Neurospora crassa*, MtCLR-4 plays a positive role in regulating cellulase gene expression by modulating its downstream targets, MtCLR-2 and MtXyr1, and the cAMP signaling pathway [23]. MtTRC-1 functions as a transcriptional activator, regulating cellulase production by modulating the expression of the transcription factor gene *Mthac-1* and the cellobiohydrolase gene *Mtcbh-1* [24]. Recently, the Zn(II)2Cys6 transcription factor MtClr-5 was reported to be crucial for cellulose decomposition, as its deletion reduced endoglucanase activity and protein secretion under cellulolytic conditions [25]. In addition, our recent study demonstrated that the forkhead regulator MtFkh1 represses major cellulase and xylanase gene expression by directly binding to their promoter regions [17].

The transcription factor CLR-2 was first identified in *N. crassa* which is an essential regulator of cellulase, but not hemicellulase gene expression [26]. The deletion of *clr-2* caused severe growth defects and completely abolished cellulase activity on Avicel, but not on xylan [26]. Since then, homologs of NcCLR-2 were fully characterized in other filamentous ascomycete fungi. The *Aspergillus nidulans* mutant carrying a disruption of *clrB*, the ortholog of *clr2*, failed to elicit cellulase gene expression and lost cellulolytic activity during growth on cellulose [26]. Similarly, the ClrB (homolog of CLR-2) is indispensable in the production of cellobiohydrolases and endoglucanases in *Aspergillus niger* [27, 28]. A recent study further showed the involvement of *A. niger* ClrB in the utilization of xyloglucan and galactomannan [29]. Also, ClrB acts as an activator of the cellulolytic gene expression in *Penicillium oxalicum* [30, 31]. In *Aspergillus oryzae*, the CLR-2 ortholog (ManR) was reported as a regulator of both mannanolytic and cellulolytic enzyme genes [32, 33]. However, the homologue of CLR-2 was described in *Trichoderma reesei* and *Talaromyces cellulolyticus* but had only a minor impact on cellulase activity [34-36]. These results indicate both similarities and differences in the functions of NcCLR-2 orthologs. In our previous analysis of the *M. thermophila* transcriptome profiling data, we noted that *Mtclr-2* (*MYCTH_38704*), the homolog of *N. crassa clr-2*, was highly upregulated under cellulosic conditions [17], implying that this gene may play roles in cellulose degradation. Indeed, the regulator MtCLR-2 has been found to be important for cellulase expression [37]. However, the detailed molecular

basis of its role in the cellulase expression has still not been fully uncovered.

In the present study, we further characterized the function of MtCLR-2 in cellulose utilization in *M. thermophila*. By a combination of molecular genetic approaches and comparative transcriptomic analyses, we found that MtCLR-2 positively regulates cellulase production by regulating the expression of the major endoglucanase gene (*egl2*) and β-glucosidase gene (*bgl1*) by directly binding to their promoter regions. In addition, we also demonstrated that MtCLR-2 is involved in ribosome biosynthesis, suggesting it regulates cellulase expression at both the transcriptional and translational levels.

Results

Identification of the MtCLR-2 protein

A BLASTP search of the *M. thermophila* genome, using the *N. crassa* CLR-2 (NCU08042, NcCLR-2) protein sequence as a query, revealed MYCTH_38704 as a putative homolog of NcCLR-2, sharing 81% sequence identity with this close ortholog. The *M. thermophila Mtclr-2* (MYCTH_38704) is 2570 bp in length and contains three exons encoding a protein composed of 798 amino acids (aa) (Fig. 1). In addition, the InterPro analysis (https://www.ebi.ac.uk/interpro/) showed the presence of a typical fungal transcription factor domain (IPR007219) between residues 259 and 434 of MtCLR-2 (Fig. 1). However, compared to NcCLR-2, MtCLR-2 lacks 14 aa in its Zn(II)2Cys6 fungal-type DNA-binding domain (DBD), between residues 44 and 75, which may explain why InterPro

analysis did not detect this domain in MtCLR-2.

Positive effect of MtCLR-2 on the production of cellulase in *M. thermophila*

To confirm the influence of MtCLR-2 on cellulase induction, we constructed *Mtclr-2* deletion mutants by using CRISPR/Cas9 system (Fig. S1). The protospacer sequence targeting *Mtclr-2* was designed for gene editing (Table S1). The Cas9-U6p-*Mtclr-2*-sgRNA plasmid was co-transformed into *M. thermophila* wild-type (WT) protoplasts along with a donor DNA vector carrying the neomycin resistance gene cassette (P*gpd*-*neo*) flanked by the 5′ and 3′ homologous arms of *Mtclr-2*. Deletion of the *Mtclr-2* gene was accomplished via homologous recombination mediated by the CRISPR/Cas9 system. The obtained disruption strains were verified by genomic PCR with three specific primer pairs (Fig. S2). After 48-96 h growth in Avicel medium, the Δ*Mtclr-2* mutants displayed a marked reduction in filter paper enzyme activity (by 56% to 60%) and β-glucosidase activity (by 26% to 40%), while endoglucanase activity was almost abolished (reduced by 90% to 92%) compared with those of the WT (Fig. 2A-C). Moreover, Δ*Mtclr-2* secreted 48% to 64% less protein than the WT under cellulosic conditions (Fig. 2D), as confirmed by SDS-PAGE analysis of extracellular proteins (Fig. S3).

Meanwhile, the *Mtclr-2* overexpression strain OE-*Mtclr-2* was created, in which *Mtclr-2* was driven by the strong constitutive pyruvate decarboxylase

(MYCTH_112121) promoter P*pdc*. The positive overexpression mutant was validated by genomic PCR using specific primer set (Fig. S2). As expected, OE-*Mtclr-2* strain exhibited a significant elevation in filter paper enzyme activity (83% to 216%), β-glucosidase activity (132% to 143%), endoglucanase activity (138% to 190%), and secreted protein (150% to 293%), compared to those of the WT when cultivated on Avicel (Fig. 2A-D). These results demonstrate that MtCLR-2 is an activator of cellulase production under cellulose induction in *M. thermophila*.

Furthermore, the role of MtCLR-2 in fungal development was explored. As shown in Fig. 3A, the Δ*Mtclr-2* mutant showed similar colony phenotype to that of the WT and OE-*Mtclr-2* strains when grown on PDA and solid Avicel media. In addition, both the *Mtclr-2* disruption and overexpression strains produced comparable numbers of asexual spores to the WT after 7 days of growth on Avicel plates (Fig. 3B). These observations suggest that MtCLR-2 is dispensable for hyphal radial growth or sporulation on solid cellulose medium. However, the Δ*Mtclr-2* mutant grew poorly in liquid cellulose culture, characterized by aberrant mycelial morphology with few hyphal branches after 36 h (Fig. 3C), but exhibited normal growth in liquid glucose medium (Fig. S4), which was similar to *N. crassa* Δ*clr-2* and *A. nidulans* Δ*clrB* mutants [26]. This growth impairment implies a specific defect associated with cellulose utilization, which is in accordance with the substantially decreased cellulase production observed in the mutant Δ*Mtclr-2*.

Subcellular localization of MtCLR-2 in *M. thermophila*

To assess the subcellular localization of MtCLR-2, the *Mtclr-2* open reading frame was fused to the *gfp* (green fluorescent protein encoding gene) under the control of the *Mtpdc* promoter (Fig. S2). This expression cassette was introduced into the WT strain, generating a strain expressing MtCLR-2-GFP. After growth in both glucose and Avicel media for 36 h, the MtCLR-2-GFP signal was found to be accumulated in the nuclei across the fungal hyphae. This signal overlapped with the blue fluorescence of the nucleic acid-specific dye DAPI (Fig. 3D), confirming that MtCLR-2 localizes to the *M. thermophila* nucleus under both glucose-repressing and cellulose-inducing conditions (Fig. S5).

MtCLR-2 regulates the expression of major cellulase genes

To test whether MtCLR-2 exerts its impact on cellulase production at the transcriptional level, we analyzed the expression of cellulase genes in the WT strain and Δ*Mtclr-2* mutant using real-time quantitative reverse transcription PCR (RT-qPCR). As shown in Fig. 4, the β-glucosidase gene *bgl1* (*MYCTH_66804*) exhibited 29% to 32% reductions in transcription levels in the *Mtclr-2* deletion strain compared with the WT during the entire induction period (24-72 h) on Avicel. Similarly, transcript level of the endoglucanase gene *egl2* (*MYCTH_86753*) was substantially decreased (by 32-fold) in Δ*Mtclr-2* mutant after 24 h of growth in Avicel medium, and was reduced by 47% to 80% at 48

and 72 h. These results agree with the observed reduction in cellulase activity in the Δ*Mtclr-2* strain. Additionally, the effects of MtCLR-2 on the transcriptional levels of key regulatory genes, including *cre1* (*MYCTH_2310085*) and *xyr1* (*MYCTH_2310145*), were examined. The transcription of *cre1* and *xyr1* was not significantly altered by the deletion of *Mtclr-2* throughout the cultivation period under cellulose-inducing conditions (Fig. 4). These observations imply that MtCLR-2 influences cellulase production primarily through regulating cellulase gene transcription.

MtCLR-2 binds to the promoter regions of *Mtbgl1* and *Mtegl2* in a zinc-dependent manner

To determine whether MtCLR-2 directly regulates the expression of *bgl1* and *egl2*, electrophoretic mobility shift assays (EMSAs) were performed. Given that MtCLR-2 lacks 14 aa within its DBD compared to NcCLR-2, we wondered whether this loss affects its DNA-binging capability. To answer this question, Strep II-fused DNA binding domain of MtCLR-2 (MtCLR-$2_{30\text{-}89}$) and MtCLR-$2_{(30\text{-}89)+14aa}$, which restores the missing 14 aa, were expressed and purified from *E. coli* BL21(DE3) (Fig. S6). DNA probes corresponding to the promoter regions of *bgl1* (P2, − 650 to − 300) and *egl2* (P2, − 650 to – 300; P3, − 1000 to − 600) were obtained by PCR. In the initial EMSAs, neither MtCLR-$2_{30\text{-}89}$ nor MtCLR-$2_{(30\text{-}89)+14aa}$ exhibited detectable binding to the upstream regions of *bgl1* or *egl2* (Fig. 5A-B). Considering that MtCLR-2 is a predicted Zn(II)2Cys6-type TF, we

hypothesized that zinc ions may be required for its DNA-binding activity. To test this, zinc ions were supplemented in the EMSA reaction buffer. Under these conditions, both MtCLR-$2_{30\text{-}89}$ and MtCLR-$2_{(30\text{-}89)+14aa}$ bound to the promoter regions of *bgl1* and *egl2* and the size of protein-DNA complex increased along with increasing amounts of MtCLR-$2_{30\text{-}89}$ and MtCLR-$2_{(30\text{-}89)+14aa}$ (Fig. 5A-B). These findings suggest that MtCLR-2 binds its target genes in the presence of zinc ions and the absence of the 14 aa in its DBD has no impact on its ability to recognize and bind target promoters.

Previous ChIP-seq (chromatin immunoprecipitation and next-generation sequencing) analysis revealed a conserved $CGG_{N11}CCG$ motif in the upstream regions of NcCLR-2-bound genes, which is nearly identical to the DNA-binding motif of its closest paralog, Gal4p, in *Saccharomyces cerevisiae* [38]. To determine whether MtCLR-2 recognizes a similar motif, we searched for the promoter regions *bgl1*-P2, *egl2*-P2, and *egl2*-P3. The conserved $CGG_{N11}CCG$ sequences were found in all these promoters, with *egl2*-P2 and *egl2*-P3 sharing identical motif fragments within their overlapping region (Fig. 5C). Additionally, the promoter region of *xyn1* (P1, −350 to −1), which lacks the $CGG_{N11}CCG$ motif, was used as a negative control. The EMSA results showed that MtCLR-$2_{30\text{-}89}$ did not form a protein–DNA complex with the *xyn1* promoter, regardless of the presence of zinc ions (Fig. S7). Thus, MtCLR-2 may identify and bind the $CGG_{N11}CCG$ motif in the promoter regions of its target genes, analogous to its homolog NcCLR-2.

Transcriptomic analysis of the *Mtclr-2* deletion mutant on Avicel

To obtain a genome-wide understanding of the molecular mechanism by which MtCLR-2 regulates cellulase production, transcriptional profile analysis was performed using the Δ*Mtclr-2* mutant grown on Avicel with the WT as comparison strain. When compared to WT, transcript levels of 2228 genes were clearly altered in mutant Δ*Mtclr-2* after 48 h of growth, with 1323 genes showing significantly decreased transcription and 905 genes displaying substantial upregulation (Fig. 6A and Table S2). A Gene Ontology (GO) analysis revealed that these differentially expressed genes (DEGs) in Δ*Mtclr-2* were enriched in the functional categories of cytosolic ribosome, polysaccharide metabolic process, and cellulose binding (Fig. 6B), in accordance with the phenotypes observed in Δ*Mtclr-2* in response to cellulose.

Comparative transcriptomic analysis revealed that three endoglucanase genes including *egl2*, *MYCTH_52068*, and *MYCTH_111372*, were remarkably downregulated in Δ*Mtclr-2* in comparison to WT, except for *MYCTH_116157* (Fig. 6C), which was in line with the endoglucanase secretion phenotype when exposed to Avicel. Three intracellular β-glucosidase genes (*MYCTH_115968*, *MYCTH_62925*, and *MYCTH_38200*) showed lower expression levels by the deletion of *Mtclr-2*. Likewise, the transcript levels of two extracellular β-glucosidase genes, *bgl1* and *MYCTH_58882*, were reduced by approximately 25% ($\log_2$ fold change = – 0.42 and – 0.41, respectively) in the Δ*Mtclr-2* mutant, which

was consistent with RT-qPCR results showing lower transcript of *bgl1* in the mutant strain, although the expression changes did not reach the strict differential analysis criteria. In addition, nine genes encoding LPMOs (AA9 family) exhibited lower transcription levels in the Δ*Mtclr-2* mutant than in the WT, except for *MYCTH_2311323* (Fig. 6C). Among these, MtLPMO9B (MYCTH_80312), MtLPMO9C (MYCTH_100518), MtLPMO9D (MYCTH_92668), and MtLPMO9J (MYCTH_79765), were found to be active against cellulose [39-41], and MtLPMO9I (MYCTH_46583) was shown to have strong synergistic effects with endoglucanase, resulting in elevated enzymatic hydrolysis yields toward cellulose [42]. Similar observation was reported in *N. crassa*, where disruption of *Ncclr-2* led to decreased expression of several secreted endoglucanase genes and one predicted intracellular β-glucosidase gene as well as one extracellular β-glucosidase gene [26, 43], while its constitutive expression caused the upregulation of several LPMO-encoding genes [38], confirming the conserved role of CLR-2 orthologs in regulating genes involved in cellulose decomposition.

Besides these cellulose degrading genes, 56 genes encoding putative transcription factors (TFs) were also observed showing altered expression levels, with 19 genes being downregulated and 37 genes being upregulated in the Δ*Mtclr-2* mutant (Fig. 6C). The majority of these TFs can be classified into Fungal Zn(II)2Cys6, Fungal_TF, and Zinc finger C2H2 families. Of these, the gene encoding CLR-4 (MYCTH_2296492), which positively regulates cellulase

gene expression [23], was downregulated (log2 fold change = – 1.02) in the absence of *Mtclr-2*. In contrast, one gene encoding AmyR (MYCTH_2301920), a repressor of cellulase production [44], was highly induced in strain Δ*Mtclr-2* ($\log_2$ fold change = 1.83). Therefore, the downregulation of *Mtclr-4* and upregulation of *MtamyR* may partially account for the reduced cellulase production seen in the Δ*Mtclr-2* mutant. Consistent with the RT-qPCR analysis above, the essential regulatory genes *Mtcre1* and *Mtxyr1* displayed no differential expression between Δ*Mtclr-2* and WT strains.

Genes encoding predicted sugar transporters were also differentially expressed in the *Mtclr-2* disruption strain (Fig. S8). Among 15 genes annotated as transporters for glucose, xylose, cellodextrin, cellobionic acid, or other sugars, two genes increased their transcription in Δ*Mtclr-2*, whereas the remaining genes decreased. Notably, *MYCTH_2302958* and *MYCTH_84164*, showed transcriptional changes, with the former downregulated ($\log_2$ fold change = −4.7) and the latter upregulated ($\log_2$ fold change = 2.3). These two genes encode proteins that share 55% and 54% sequence similarity, respectively, with cellobionic acid transporter CBT-1 in *N. crassa*, which suppresses cellulase induction on both cellobiose and Avicel [45, 46]. Whether the altered expression of these putative *cbt-1* homologs contributes to the decreased cellulase induction observed in the Δ*Mtclr-2* mutant remains to be elucidated.

Interestingly, a set of ribosomal protein genes exhibited reduced transcript abundance in the mutant Δ*Mtclr-2*, including 25 potential genes encoding 40S

small ribosomal subunit proteins and 36 encoding 60S large ribosomal subunit proteins (Fig. 6D). Additionally, seven genes encoding putative mitochondrial ribosomal proteins, including three small ribosomal protein genes and four large ribosomal protein genes, were also downregulated upon *Mtclr-2* disruption (Fig. 6D). The transcriptional repression of ribosomal protein genes has not been reported in other fungal species where the roles of MtCLR-2 homologs have been explored. These findings suggest that MtCLR-2 may regulate the production of cellulases not only at the transcriptional level but potentially also at the translational level.

Discussion

Myceliophthora thermophila is a thermophilic fungus able to secrete a complete set of thermostable enzymes involved in plant biomass degradation, including cellulases and xylanases. In recent years, this fungus has been developed into a platform to produce industrially relevant enzymes [47, 48] and used as a model system for exploring basic fungal cell biology, such as the mechanism of expression and secretion of lignocellulolytic enzymes [24, 49, 50]. A few transcription regulators related to lignocellulose deconstruction have been identified in this fungus, including MtFkh1, MtXyr1, MtCre1, MtClr-4, and MtTrc-1 [17, 21-24]. However, more transcription factors involved in inducing the expression of lignocellulolytic enzyme-encoding genes in *M. thermophila* remain to be elucidated. In this paper, we present the molecular basis underlying

cellulase expression regulated by MtCLR-2, which is the ortholog of NcCLR-2 in *N. crassa*. The assay of cellulase production of *Mtclr-2* deletion and overexpression strains indicated that MtCLR-2 serves as an activator of cellulase production. The disruption of this nuclear localized transcription factor MtCLR-2 drastically decreased cellulolytic enzyme production, whereas the overexpression of MtCLR-2 resulted in cellulase enzyme activities that were elevated approximately two-fold compared with the WT when *M. thermophila* was grown on cellulose. This role was supported by our RT-qPCR and transcriptomic analyses, which uncovered downregulated expression of the major endoglucanase and β-glucosidase genes and several genes encoding crucial LPMOs (AA9 family) in the Δ*Mtclr-2* strain. In addition, the severely affected growth of Δ*Mtclr-2* in liquid cellulose medium but normal growth in glucose culture suggested that MtCLR-2 is specifically involved in cellulose catabolism. However, no obvious difference was observed in the cellobiohydrolase activity between the Δ*Mtclr-2* and WT strains for growth on Avicel (Fig. S9), despite transcriptomic data revealed the downregulation of five cellobiohydrolase genes and upregulation of one cellobiohydrolase gene in the Δ*Mtclr-2* mutant (Fig. S8), indicating a self-equilibrating mechanism that modulates production of cellulase. Overall, herein, we provide a potential target for rational fungal strain engineering for hyperproduction of cellulase.

Previous studies showed that the absence of *Ncclr-2* resulted in no detectable endoglucanase activity and almost abolished secreted protein production when

N. crassa was grown on cellulose [26]. Our research also demonstrated that MtCLR-2 has a similar role in the regulation of endoglucanase and total protein secretion in cellulose-induced cultures. Also, the considerably reduced endoglucanase activity was reported on *A. nidulans* Δ*clrB* [26] and *P. oxalicum* Δ*clrB* mutants [30]. Accordingly, significant decrease in expression levels of the major endoglucanase genes was observed in the Δ*Mtclr-2* strain, which was in accordance with findings from *N. crassa*, *A. nidulans*, *A. niger*, *P. oxalicum*, and *A. oryzae*, where the deletion of *Mtclr-2* orthologs caused the downregulation of the essential endoglucanase genes under cellulosic conditions [26-28, 30, 33, 43]. These observations clearly indicate the conserved role of CLR-2 homologs in endoglucanase gene regulation. Similar to *N. crassa* CLR-2 and *A. nidulans* ClrB, several important LPMO-encoding genes were downregulated by the deletion of *Mtclr-2* in response to Avicel, the majority of which have been found to exert oxidative roles toward cellulose [43]. Regarding β-glucosidase and cellobiohydrolase gene expression, differences in function of CLR-2 homologs have been reported. For example, the Δ*clrB* mutant of *P. oxalicum* exhibited reduced cellobiohydrolase activity [30] and enhanced β-glucosidase activity when exposed to Avicel [31], which was consistent with the downregulation of the main cellobiohydrolase genes and upregulation of the major β-glucosidase genes. In contrast, the present study showed that the disruption of *Mtclr-2* decreased β-glucosidase activity while having no impact on cellobiohydrolase production, highlighting the complex regulatory networks in which CLR-2

orthologs are involved in regulating the expression of different cellulase enzymes. In addition, overexpression of *TRIREDRAFT_26163*, the *T. reesei* homolog of *Ncclr-2*, resulted in only a slight elevation in cellulase production [34]. Similarly, in *T. cellulolyticus*, the loss of *tclB2*, which is the homolog of *Ncclr-2*, exhibited minor effects on cellulase activity when cultivated on cellulose [35]. Therefore, the role of CLR-2 homologs in cellulose utilization appears to be partially conserved among filamentous fungi.

The production of cellulolytic enzymes in fungi is tightly regulated by transcription factors [18, 19]. According to our transcriptomic data analysis, transcription factors involved in the regulation of cellulase gene expression, including *Mtclr-4* [23] and *MtamyR* [44], showed altered expression levels by the deletion of *Mtclr-2*, implying that MtCLR-2 regulates cellulase production by modulating transcript levels of regulatory proteins. These targeted transcription factors could function as secondary regulators, enabling more fine-tuned gene expression [38]. In *N. crassa*, *xlr-1*, which encodes a key transcription factor that regulates the expression of hemicellulolytic enzyme genes and is necessary for utilization of hemicellulose, was downregulated in the Δ*clr-2* strain [26]. However, this is not the case for *M. thermophila*, where the transcription of *Mtxyr1*, the homolog of *xlr-1*, remained unchanged in the mutant Δ*Mtclr-2* under conditions of cellulose exposure. In addition, CLR-1, another predominant regulator of cellulolytic enzymes in *N. crassa*, is essential for *clr-2* expression, since the expression of *clr-2* was abolished in the Δ*clr-1* mutant, while that of

clr-1 was not influenced by the disruption of *clr-2* during growth on Avicel [26]. Further DNA motif analysis of the bound genes revealed that CLR-1 binds to the promoter region of *clr-2* under cellulosic conditions [38]. Similar to *N. crassa clr-2*, *Mtclr-2* is not required for the expression of *Mtclr-1* (*MYCTH_2298863*), the *Ncclr-1* ortholog in *M. thermophila*, revealed by the transcriptome data showing the unaffected expression level of *Mtclr-1* in the Δ*Mtclr-2* mutant. Whether *Mtclr-2* is bound and regulated by MtCLR-1 needs to be further investigated. Unlike the results observed with *Ncclr-2* and *Mtclr-2*, the expression of *clrA*, the ortholog of *clr-1*, which is involved in cellulose degradation, was reported to be (partially) dependent on ClrB in *A. niger* [29], suggesting divergences between the regulatory networks coordinating lignocellulose deconstruction and utilization among different filamentous fungi.

In *N. crassa*, CLR-2 binds to 5′-CGGN$_{11}$CCG-3′ motifs in the promoter regions of its regulon [38]. Combined ChIPseq and RNAseq analyses identified that 54 genes were both bound by CLR-2 and dependent on it for their expression [38]. Our data showed that *egl2* and *bgl1* were consistently downregulated at all examined time points in the *Mtclr-2* disruptant, indicating the high dependence of MtCLR-2 for activation of their expression. Further EMSA analysis demonstrated that MtCLR-2 can directly bind to the promoter regions of *egl2* and *bgl1* in a zinc-dependent manner, although the lack of 14 aa in its DNA-binding domain compared to NcCLR-2. Like NcCLR-2, the 5′-CGGN$_{11}$CCG-3′ sequence was found in the upstream regions of both *egl2* and *bgl1*, indicating

that MtCLR-2 might also bind this motif to regulate its target genes. In addition, the 5′-CGGN$_{11}$CCG-3′ motif was identified in the promoter regions of *Mtlpmo9B*, *Mtlpmo9C*, and *Mtlpmo9D*, but was absent in those of *Mtcre1* and *Mtxyr1*. This observation is consistent with the expression patterns of these genes in the Δ*Mtclr-2* mutant revealed by both RT-qPCR and/or transcriptomic analyses, further supporting the regulatory importance of this motif. It has been shown that ClrB in *A. nidulans* can bind to 5′-CGGN$_8$CCG-3′ motifs in the promoter region of the β-mannosidase gene *mndB* in the presence of zinc ions, and loss of either one of the CGG or CCG triplet completely abolished protein–DNA interaction [51]. Likewise, *eglA* and *bgl4* were downregulated in the *A. niger* Δ*clrB* strain when grown in soybean hull or guar gum liquid media, and both gene possess predicted ClrB consensus binding sites (5′-CGGN$_8$CCG-3′) in their upstream regions [29]. These experimentally confirmed or putative binding sequences of ClrB in *A. nidulans* and *A. niger* are highly similar to the predicted binding site of MtCLR-2 identified in this study. Nevertheless, *A. nidulans* ClrB does not bind directly to the *eglB* promoter, which contains one 5′-CGGN$_8$CCG-3′ site. Instead, it is recruited to a CeRE-like (cellulose-responsive element-like) sequence upstream of *eglB*, which also contains a CCG triplet, through the assistance of McmA, a SRF (serum response factor)-type MADS box protein that regulates both cellulase production and asexual/ sexual development [51]. This implies a different type of ClrB-mediated regulatory system. Whether MtCLR-2 interacts with unknown cofactors to facilitate its binding and regulatory

functions remains to be determined.

An unexpected finding of this study is that 68 genes encoding ribosomal proteins were downregulated in the absence of *Mtclr-2*, which may explain dramatically decreased protein secretion in the cultures of strain Δ*Mtclr-2* cultivated on cellulose. Studies in yeast indicate the activation of ribosomal protein genes (RPGs) transcription is accomplished by several partly specialized regulatory factors that are not unique to RPG promoters [52]. The most prominent transcription factors are Rap1 (Repressor/activator protein 1), Fhl1 (Forkhead-like 1), and Ifh1 (Interacts with forkhead 1), which form a regulatory complex at the majority of RPG promoters [53]. In addition, the high mobility group (HMG)-box protein Hmo1 binds to around half of the promoters of RPGs bound by Rap1-Fhl1-Ifh1 complex [54]. However, the homologs of these identified transcription factors regulating RPGs are absent in *M. thermophila*. On the other hand, the TOR (target of rapamycin) pathway has been demonstrated to be essential for the transcription of RPGs in *S. cerevisiae*, in which the key genes are *Tor1* and *Tor2* [55]. When the TOR pathway is inactivated by nutrient starvation or by treatment of cells with rapamycin, the transcript level of RPGs is downregulated [55, 56]. It has also been proposed that the transcription factor Sfp1, which acts downstream of the TOR pathway, modulates the transcription of RPGs in response to changes in nutrient availability [56, 57]. While orthologs of Tor1/Tor2 (*MYCTH_2307294*) and Sfp1 (*MYCTH_2294631*) are present in *M. thermophila*, their expression levels did not

differ significantly between the Δ*Mtclr-2* and WT strains (log_2 fold change = −0.58 and 0.03, respectively). In *N. crassa*, it has been reported that the disruption of *cpc-1*, which encodes a bZIP transcription factor known as the cross pathway control-1(CPC1), resulted in elevated expression of 37 ribosomal protein genes, suggesting that CPC1 acts as a repressor of ribosomal protein gene expression [58]. In our transcriptomic analysis, *MYCTH_2315566*, the homolog of *cpc-1* in *M. thermophila*, was upregulated in the Δ*Mtclr-2* mutant (log_2 fold change = 1.63), which may partially be responsible for the observed downregulation of genes involved in ribosome biogenesis. It is also possible that, in the loss of *Mtclr-2*, fungal cells reduced the transcription of ribosomal protein genes as an adaptive response to nutrient limitation during cultivation on cellulose. Since the Δ*Mtclr-2* mutant is unable to secrete sufficient cellulases to efficiently degrade cellulose into monosaccharides and/or oligosaccharides, it likely experiences carbon scarcity. In such scenario, the downregulation of ribosome biogenesis may serve as a strategy to conserve energy for basic cellular functions, given that ribosome synthesis is one of the most energy-consuming processes in the cell [55, 57]. The growth defect of Δ*Mtclr-2* on cellulose, but not on glucose, suggests that the downregulation of ribosomal protein genes and the resulting secretion impairment, may be specifically associated with cellulose utilization. It has been shown that ribosomal protein gene expression is strongly induced when yeast cells are transferred from unfavorable carbon source to glucose-containing medium [55, 59, 60]. Moreover,

in *N. crassa*, the rate of ribosomal protein synthesis increased considerably after a nutritional upshift from acetate to glucose, but was severely repressed upon a shift from glucose to glycerol [61]. Similar observation was reported in *S. cerevisiae*, where transcript levels of 90 ribosomal proteins were reduced in response to amino deficiency [62]. Likewise, in *N. crassa*, 67 genes encoding predicted ribosomal proteins were downregulated under amino acid starvation [58]. These studies indicate that the altered expression of ribosomal protein genes represents a common response to nutritional changes. However, the precise mechanism by which MtCLR-2 mediates the regulation of ribosomal protein gene expression under cellulolytic conditions merits further investigation.

Conclusions

MtCLR-2 was identified as a transcriptional activator that regulates cellulase production by directly binding to the promoter regions of *egl2* and *bgl1* to modulate their expression. Additionally, MtCLR-2 was found to be associated with ribosomal protein biosynthesis. This study not only provides insights into the regulatory network for cellulase gene expression but also highlights MtCLR-2 as a promising target for rational genetic engineering to enhance cellulolytic enzyme production in *M. thermophila*.

Materials and methods

Strains and culture conditions

Myceliophthora thermophila (ATCC 42464) was used as parental strain throughout this work. Conidial suspensions of *M. thermophila* strains were prepared by culturing them on potato dextrose agar (PDA) incubated at 45℃ for 7 days. The spores were harvested and suspended in 0.2% (v/v) Tween-80 solution and counted using a hemocytometer. For DNA extraction, the fungi were grown in Mandels medium containing 2% (w/v) glucose as carbon source, incubated at 45°C with shaking at 150 rpm for 36 h [17]. For enzymatic activity assays, RT-qPCR, and comparative transcriptome analyses, mycelia were first pre-cultured from conidia in Mandels medium containing 2% (w/v) glucose for 36 h (final concentration, 1×10^6 spores mL^{-1}). The mycelia were then washed with carbon-free Mandels medium, and an equal amount (0.55 g) of wet mycelia was transferred into 50 mL of Mandels medium supplemented with 2% (w/v) Avicel (Sigma-Aldrich, Darmstadt, Germany), and incubated at 45°C with shaking at 150 rpm for 48–96 h. For fungal colony morphology and conidiation assays, 1.5 μL of spore suspensions (1×10^7 mL^{-1}) from *M. thermophila* strains were inoculated onto the center of PDA solid plates containing 1% (w/v) Avicel and incubated at 45°C for 3–7 days. For growth observation in liquid culture, conidia of fungal strains were added to 50 mL Mandels medium supplemented with 2% (w/v) glucose or 2 % (w/v) Avicel (final concentration, 1×10^6 conidia mL^{-1}), and grown at 45°C for 36 h. Fungal mycelia cultured in liquid shaking flasks were either subjected to macroscopic observation or harvested for microscopic

analysis using light microscopy.

Escherichia coli DH5α was used for plasmid construction and propagation, cultured at 37℃ in Luria-Bertani (LB) medium supplemented with ampicillin (100 μg mL^{-1}).

Plasmid construction

All the primer sequences used in this study are listed in Table S1. For the knockout of *Mtclr-2* (MYCTH_38704) using the CRISPR/Cas9 system, the Cas9-U6p-*Mtclr-2*-sgRNA expression cassette was constructed as described previously [17]. Specific sgRNA target site for *Mtclr-2* was identified using the sgRNACas9 tool with minimum off-target effects [63]. The DNA fragments, including the U6 promoter of *M. thermophila*, and the target DNA sequence that fused with sgRNA scaffold were obtained by PCR using the pFC332-Cas9-U6p-sgRNA scaffold vector as the template [17] and cloned into the pFC332 vector to create the plasmid Cas9-U6p-*Mtclr-2*-sgRNA. To construct the donor DNA vector, the 5′ and 3′ flanking segments of *Mtclr-2* were separately amplified from *M. thermophila* genomic DNA by PCR, fused with the selectable marker cassette P*gpd-neo* from a pBC-*neo* plasmid [64], and inserted into the HindIII and EcoRI sites of pUC19 plasmid to generate Donor-*Mtclr-2-neo* using One Step Cloning Kit (Vazyme Biotech, Nanjing, China).

To generate *Mtclr-2* overexpression vector, the gene-coding region of *Mtclr-2* was amplified from genomic DNA and ligated into pUC19-P*pdc*-T*gpdA*-*hph*

plasmid at the NotI and XbaI sites, under the control of the strong constitutive *Mtpdc* (MYCTH_112121, pyruvate decarboxylase) promoter of *M. thermophila*. Similarly, for intracellular localization analysis of MtCLR-2, the PCR-amplified *Mtclr-2* coding region without the stop codon and the *gfp* (green fluorescent protein) gene were assembled and cloned into the NotI and XbaI sites of pUC19-P*pdc*-T*gpdA*-*hph* plasmid to generate the *Mtclr-2-gfp* cassette.

Transformation of *Myceliophthora thermophila* protoplasts

Protoplast preparation and transformation of *M. thermophila* was carried out following previously reported methods [17]. Possible transformants for gene deletion or overexpression in *M. thermophila* were screened for resistance to neomycin and hygromycin B (75 μg mL^{-1} hygromycin B combined with 100 μg mL^{-1} G418) or to hygromycin B alone (75 μg mL^{-1}) after 4-5 days of incubation on PDA plates. Positive transformants were verified by PCR analysis with different specific primer pairs (Table S1), followed by sequencing.

Protein and enzyme activity assays

The extracellular protein concentration in the culture supernatant was measured using a Modified Bradford Protein Assay kit (Sangon Biotech, Shanghai, China) based on 595 nm absorbance. A 20 μL aliquot of culture supernatant was loaded on a 10% polyacrylamide gel (PAGE Gel Quick Preparation Kit, Yeasen Biotech, Nanjing, China) to analyze the proteins by SDS-PAGE (Sodium Dodecyl Sulfate

Polyacrylamide Gel Electrophoresis). Cellulase activities, including filter paper cellulase (FPase), endoglucanase (CMCase), β-glucosidase (pNPGase), and cellobiohydrolase (pNPCase), were determined as previously described [17]. One unit (U) of enzymatic activity was defined as the amount of enzyme that releases 1 μmol of either glucose or *p*-nitrophenol (*p*NP) from the substrate per minute under standard assay conditions.

Fluorescence microscopy examination

To determine subcellular localization of MtCLR-2 in *M. thermophila*, MtCLR-2-GFP positive transformants were inoculated into Mandels medium containing 2% (w/v) glucose or 2% (w/v) Avicel as the sole carbon source and incubated for 36 h at 45 °C. The mycelia were collected and incubated in darkness with 5 mg L^{-1} 4′,6-diamidino-2-phenylindole (DAPI) solution for 15 min, and washed with PBS solution three times. Fungal mycelia were observed under an Olympus BX53 fluorescence microscope, and the images were processed using Olympus cellSens Standard software.

Real-time quantitative PCR

Total RNA was extracted from frozen mycelia using an RNA extraction kit TransZol Up (TransGen Biotech, Beijing, China) according to the manufacturer's instructions. Reverse transcription was performed using the HiScript III RT SuperMix kit with gRNA wiper (Vazyme Biotech, Nanjing, China) following the

manufacturer's protocols. Quantitative PCR was performed with Hieff UNICON Universal Blue qPCR SYBR Green Master Mix (Yeasen Biotech, Shanghai, China), as described in our previous study [17]. The transcript level of each gene was estimated by the $2^{-\Delta\Delta CT}$ method [65] with the *actin* gene (MYCTH_2314852) as an internal control. The relative transcript level was determined by calculating the radio of the transcript level in the *Mtclr-2* deletion mutant to that in the WT control, which was set as 100 %. Each reaction was conducted in triplicate.

Expression and purification of the MtCLR-2 DNA-binding domain

The three exon-coding sequences of *Mtclr-2* were first obtained by amplifying from *M. thermophila* genomic DNA using the primer sets shown in Table S1. These fragments were then assembled and inserted into the HindIII stie of pET-51b to generate pET-51b-MtCLR-$2_{1\text{-}798}$ plasmid. Due to the short length and limited expression of the MtCLR-2 DNA-binding domain (amino acids 44 to 75), an extended fragment comprising amino acids 30 to 89, which includes the core domain and 14 additional residues on both the N- and C-terminal sides, was selected for expression. To express the MtCLR-2 DNA-binding domain, the sequence encoding the amino acids 30 to 89 was amplified by PCR from the pET-51b-MtCLR-$2_{1\text{-}798}$ plasmid and was ligated into the pET-51b to create the pET-51b-MtCLR-$2_{30\text{-}89}$ recombinant plasmid. The codon optimized pUC57-MtCLR-$2_{1\text{-}272}$ vector, containing DNA sequence that encodes amino acids 1 to 272, was synthesized by IGE Biotechnology (Guangzhou, China). This plasmid includes an

additional 14 amino acids that were absent in the MtCLR-2 DBD compared to the NcCLR-2 DBD. For the expression of the MtCLR-2 DBD that restores the missing 14 amino acids (residues 30 to 103), the corresponding DNA sequence was amplified by PCR using the pUC57-MtCLR-$2_{1\text{-}272}$ plasmid as the template and was inserted into HindIII-digested pET-51b to obtain the recombinant vector pET-51b-MtCLR-$2_{(30\text{-}89)+14aa}$. The recombinant plasmids were subsequently introduced into *E. coli* BL21(DE3) for protein expression, and the Strep II-tagged proteins were purified and verified as described previously [17].

Electrophoretic mobility shift assays (EMSAs)

EMSAs were carried out as previously reported [17]. Briefly, promoter regions of *bgl1* (MYCTH_66804, P2, − 650 to − 300) and *egl2* (MYCTH_86753, P2, − 650 to – 300; P3, − 1000 to − 600) were amplified from *M. thermophila* genomic DNA using specific primers shown in Table S1. For each EMSA reaction, varying amounts of purified recombinant MtCLR-$2_{30\text{-}89}$ (0-0.04 μg) or MtCLR-$2_{(30\text{-}89)+14aa}$ (0-0.1 μg) were incubated with a fixed amount (100 ng) of the corresponding DNA probe in solution containing Gel-Shift Binding Buffer (Beyotime Biotech, Shanghai, China) with or without $ZnSO_4$ at a final concentration of 25 mM, at 25°C for 30 min. After incubation, the protein-DNA complexes and free DNA were separated by electrophoresis on native 6 % polyacrylamide gels with 0.5 ×TBE running buffer at 110 V for 70 min at 4°C and finally stained using YeaRed Nucleic Acid Gel Stain (Yeasen Biotech, Shanghai, China). The promoter region

of *xyn1* (MYCTH_112050, P1, −350 to −1) was used as a negative control.

Analysis of transcriptomic data

The quality and quantity of total RNA extracted from *M. thermophila* wild-type strain, and its mutant were assessed using agarose gel electrophoresis and a NanoDrop 2000 Spectrophotometer (Thermo Scientific, Waltham, MA, USA). High-quality purified RNA was used for RNA sequencing (RNA-seq) on the Illumina NovaSeq 6000 platform, performed by Gene Denovo Biotechnology Corporation (Guangzhou, China). Clean reads were generated and mapped to the *M. thermophila* ATCC 42464 genome using HISAT2 v2.4 [66]. Gene expression levels were calculated using RSEM software [67], with transcript abundance represented as fragments per kilobase of transcript per million mapped reads (FPKM). Differential gene expression analysis was conducted using DESeq2 [68], with criteria set at an absolute fold change > 2 and an adjusted *P*-value (padj) < 0.05. The detailed data are shown in Table S2. Gene Ontology (GO) enrichment analysis was performed using OmicShare tools (https://www.omicshare.com/tools). All differentially expressed genes (DEGs) were mapped to GO terms in the Gene Ontology database (http://www.geneontology.org/), and significantly enriched GO terms (*P*-value < 0.05) were identified via a hypergeometric test against the *M. thermophila* genome background. The raw transcriptome sequencing data have been deposited in the Gene Expression Omnibus (GEO) database under the accession

number GSE305312 at the National Center for Biotechnology Information (NCBI).

Fig. 1 Schematic representation of the *Mtclr-2* gene structure and the predicted functional domains of the MtCLR-2 protein. MtCLR-2 lacks 14 aa in its putative Zn(II)2Cys6 fungal-type DNA-binding domain compared to NcCLR-2. NcCLR-2, *N. crassa* CLR-2.

Fig. 2 Cellulase activities and protein production of *M. thermophila* WT strain, Δ*Mtclr-2* mutants, and OE-*Mtclr-2* strain. **(A)** Filter paper cellulase (FPase) activity. **(B)** Endoglucanase (CMCase) activity. **(C)** β-glucosidase (pNPGase) activity. **(D)** Extracellular protein concentration. These *M. thermophila* strains were pre-grown in glucose for 36 h and then transferred to 2% (w/v) Avicel medium and cultured for 48-96 h. $^{**}p < 0.01$, and $^{***}p < 0.001$ indicate significant differences between the WT and Δ*Mtclr-2* mutants or OE-*Mtclr-2* strain (Two-way ANOVA), ns indicates not significant. Error bars represent the SD from three replicates.

Fig. 3 Phenotypic analyses of *M. thermophila* WT, Δ*Mtclr-2*, and OE-*Mtclr-2* strains and subcellular localization of MtCLR-2 protein. **(A)** Colony phenotype on PDA and 1% (w/v) Avicel solid plates after 3 (PDA) or 4 days (Avicel) of growth

at 45°C. **(B)** Quantitative determination of conidiation on plates containing 1% (w/v) Avicel cultivated at 45°C after 7 days. ns indicates no noticeable differences between WT and Δ*Mtclr-2*, or OE-*Mtclr-2* strains (Student's t tests). Error bars represent the SD from three replicates. **(C)** Microscopic observations of fungal mycelia after 36 h of cultivation in liquid shaking flasks containing 2% (w/v) Avicel as the sole carbon source. Aberrant hyphal branches in the Δ*Mtclr-2* strain are indicated by red arrows. Scale bar = 10 μm. **(D)** Subcellular location of MtCLR-2 in *M. thermophila*. MtCLR-2-GFP strain was cultivated in liquid medium containing 2% (w/v) glucose as the sole carbon source at 45°C for 36 h. Scale bar = 20 μm.

Fig. 4 Relative transcription levels of major cellulase genes *bgl1* and *egl2* as well as the regulatory genes *cre1* and *xyr1* in *M. thermophila* WT and Δ*Mtclr-2* strains. Strains were pre-grown in glucose for 36 h, washed and transferred to 2% (w/v) Avicel medium and cultivated for 24, 48, and 72 h. The expression level of each gene in Δ*Mtclr-2* was normalized to the level of the corresponding gene in WT. $^{**}p < 0.01$, and $^{***}p < 0.001$ represent significant differences between the Δ*Mtclr-2* and WT strains (Two-way ANOVA), ns indicate no significant difference. Error bars represent the SD from three replicates.

Fig. 5 Electrophoretic mobility shift assays (EMSAs) of the interactions between MtCLR-2 and the promoter regions of major genes encoding cellulases. **(A)**

EMSAs of the binding between MtCLR-$2_{30\text{-}89}$ and the promoter regions of *bgl1* and *egl2* in the presence or absence of zinc ions. **(B)** EMSAs of the binding between MtCLR-$2_{(30\text{-}89)+14aa}$ and the promoter regions of *bgl1* and *egl2* in the presence or absence of zinc ions. The concentration of zinc ions in the reaction buffer was 12.5 mM. **(C)** Schematic diagram of the putatively conserved MtCLR-2 binding motif in the promoter regions of *bgl1* and *egl2*. MtCLR-2 may identify and bind the $CGG_{N11}CCG$ motif in the promoter regions of its target genes, box in green indicates variable N_{11} nucleotides.

Fig. 6 Comparative transcriptomic analysis of strains Δ*Mtclr-2* and WT cultivated in 2% (w/v) Avicel medium for 48 h after a shift from glucose. **(A)** Volcano plots demonstrating differentially expressed genes (DEGs) between Δ*Mtclr-2* and WT strains. Genes that were significantly upregulated and downregulated in the Δ*Mtclr-2* mutant compared to the WT are plotted in red and green, respectively. **(B)** Gene Ontology (GO) enrichment of 2228 DEGs in the biological process, cellular component, and molecular function categories. **(C)** Heatmap analysis of expression profiles for genes encoding cellulases, LPMOs, and putative transcription factors between Δ*Mtclr-2* and WT strains. **(D)** Heatmap analysis of expression profiles for genes encoding putative ribosomal proteins between Δ*Mtclr-2* and WT strains. Heatmaps show the Z-score–normalized expression levels of selected genes across the Δ*Mtclr-2* mutant and WT samples.

Supplementary Information

The online version contains supplementary material available at

Fig. S1 Schematic diagram of the deletion of *Mtclr-2* in *M. thermophila* using the CRISPR-Cas9 system. sgRNA, single chimeric guide RNA; PAM, protospacer adjacent motif; *neo*, G418 resistance gene.

Fig. S2 Genomic PCR verification of the deletion and overexpression of *Mtclr-2* in *M. thermophila*. **(A)** PCR analysis for deletion strains of *Mtclr-2*. Primer 1-F locates in P*gpdA-neo*, and Primer 1-R locates out of 3′ flanking region of *Mtclr-2*; Primer 2-F locates out of 5′ flanking region of *Mtclr-2*, and Primer 2-R is in 3′ flanking region; The primer pair 3 is used to amplify *Mtclr-2*. a, the primer pair 1; b, the primer pair 2; c, the primer pair 3; M, DL 5000 Marker; WT, *M. thermophila* wild type strain. **(B)** PCR analysis of the *Mtclr-2* overexpression strain and the *Mtclr-2-gfp* fusion strain. M, DL 5000 Marker; WT, *M. thermophila* wild type strain.

Fig. S3 SDS-PAGE analysis of the secreted proteins in *M. thermophila* WT, Δ*Mtclr-2*, and OE-*Mtclr-2* strains. These strains were grown in glucose medium for 36 h and subsequently transferred to liquid Avicel medium for 48 and 72 h. M, 10-180 kDa protein marker; WT, *M. thermophila* wild type strain.

Fig. S4 Microscopic observation of fungal growth of *M. thermophila* WT, Δ*Mtclr-2* and OE-*Mtclr-2* strains cultured in shaken liquid medium. The mycelia were harvested from liquid media containing 2% (w/v) glucose as the sole carbon source after cultivation at 45°C for 36 h. Scale bars = 10 μm.

Fig. S5 Subcellular location of MtCLR-2 in *M. thermophila*. MtCLR-2-GFP strain was cultivated in liquid medium containing 2% (w/v) Avicel as the sole carbon source at 45°C for 36 h. Scale bar = 20 μm.

Fig. S6 SDS-PAGE and LC-MS/MS analysis of purified MtCLR-$2_{30\text{-}89}$ and MtCLR-$2_{(30\text{-}89)+14aa}$ proteins. **(A)** SDS-PAGE verification of purified MtCLR-$2_{30\text{-}89}$ and MtCLR-$2_{(30\text{-}89)+14aa}$. The sample was loaded onto a 12.5% polyacrylamide gel. M, 10-180 kDa. **(B-C)** LC-MS/MS characterization of MtCLR-$2_{30\text{-}89}$ **(B)** and MtCLR-$2_{(30\text{-}89)+14aa}$ **(C)** proteins. The target protein band was excised from the gel and analyzed using LC-MS/MS assays with the PEAKS Studio 8.5 system. Approximately 99% and 91% of the amino acids of the target protein matched the theoretical amino acid sequence of the Strep II-MtCLR-$2_{30\text{-}89}$-His tag fusion protein, and Strep II-MtCLR-$2_{(30\text{-}89)+14aa}$ -His tag fusion protein, respectively.

Fig. S7 Electrophoretic mobility shift assays (EMSAs) analyzing the binding of MtCLR-2*30-89* to the promoter region of *xyn1* in the presence or absence of zinc ions.

Fig. S8 Heatmap analysis of expression profiles for genes encoding cellobiohydrolases and putative sugar transporters between Δ*Mtclr-2* and WT strains grown in 2% (w/v) Avicel medium for 48 h after a shift from glucose medium.

Fig. S9 Cellobiohydrolase (pNPCase) activity of *M. thermophila* WT and Δ*Mtclr-2* strains. Culture supernatants were collected from fungal strains cultivated on 2% (w/v) Avicel for 72 h at 45°C after a shift from glucose. Ns indicate not significant (Student's t tests). Error bars represent the SD from three replicates.

Table S1 List of PCR primers used in this study. The green bold capital nucleotides indicate the protospacer sequence of *MYCTH_38704* gene. The lowercase nucleotides represent homologous arm fragments for constructing corresponding vectors.

Table S2 Differentially expressed genes (DEGs) in *M. thermophila* Δ*Mtclr-2* strain relative to WT cultured on 2% (w/v) Avicel for 48 h.

Acknowledgements

We thank Shenzhen University and Auckland University of Technology for their

support of this study.

Author contributions

GL, DLB and JW initiated, designed, supervised this study, edited and reviewed the manuscript. YL planned and carried out experiments, interpreted experimental data, and drafted the manuscript. GL, NX and JW supported the research funding. All authors read and approved the final manuscript.

Funding

This work was supported by the Natural Science Foundation of China (22078199), Natural Science Foundation of Guangdong Province (2024B1515020034), National Key R&D Program of China (2021YFA0910800), Shenzhen Municipal Science and Technology Basic Research Program (JCYJ20200109105210448).

Data availability

All data generated or analyzed during this study are included in this published article and its supplementary information files.

Declarations

Ethics approval and consent to participate

Not applicable.

Consent for publication

Not applicable.

Competing interests

The authors declare that they have no competing interests.

References

1. Li Y, Song W, Han X, Wang Y, Rao S, Zhang Q, Zhou J, Li J, Liu S, Du G. Recent progress in key lignocellulosic enzymes: Enzyme discovery, molecular modifications, production, and enzymatic biomass saccharification. Bioresour Technol. 2022; 363:127986.
2. Gupta VK, Kubicek CP, Berrin JG, Wilson DW, Couturier M, Berlin A, Filho EXF, Ezeji T. Fungal Enzymes for Bio-Products from Sustainable and Waste Biomass. Trends Biochem Sci. 2016; 41:633-645.
3. Taha M, Foda M, Shahsavari E, Aburto-Medina A, Adetutu E, Ball A. Commercial feasibility of lignocellulose biodegradation: possibilities and challenges. Curr Opin Biotechnol. 2016; 38:190-197.
4. Frommhagen M, Westphal AH, van Berkel WJH, Kabel MA. Distinct Substrate Specificities and Electron-Donating Systems of Fungal Lytic Polysaccharide Monooxygenases. Front Microbiol. 2018; 9:1080.
5. Andlar M, Rezic T, Mardetko N, Kracher D, Ludwig R, Santek B. Lignocellulose degradation: An overview of fungi and fungal enzymes involved in lignocellulose degradation. Eng Life Sci. 2018; 18:768-778.
6. Mattam AJ, Chaudhari YB, Velankar HR. Factors regulating cellulolytic gene expression in filamentous fungi: an overview. Microb Cell Fact. 2022; 21:44.
7. Makela MR, Donofrio N, de Vries RP. Plant biomass degradation by fungi. Fungal Genet Biol. 2014; 72:2-9.
8. Berka RM, Grigoriev IV, Otillar R, Salamov A, Grimwood J, Reid I, Ishmael N, John T, Darmond C, Moisan MC, et al. Comparative genomic analysis of the thermophilic biomass-degrading fungi Myceliophthora thermophila and Thielavia terrestris. Nat Biotechnol. 2011; 29:922-927.
9. Singh B. Myceliophthora thermophila syn. Sporotrichum thermophile: a thermophilic mould of biotechnological potential. Crit Rev Biotechnol. 2016; 36:59-69.
10. Liu Q, Gao R, Li J, Lin L, Zhao J, Sun W, Tian C. Development of a genome-editing CRISPR/Cas9 system in thermophilic fungal Myceliophthora species and its

application to hyper-cellulase production strain engineering. Biotechnol Biofuels. 2017; 10:1.

11. Gu S, Li J, Chen B, Sun T, Liu Q, Xiao D, Tian C. Metabolic engineering of the thermophilic filamentous fungus Myceliophthora thermophila to produce fumaric acid. Biotechnol Biofuels. 2018; 11:323.
12. Li J, Gu S, Zhao Z, Chen B, Liu Q, Sun T, Sun W, Tian C. Dissecting cellobiose metabolic pathway and its application in biorefinery through consolidated bioprocessing in Myceliophthora thermophila. Fungal Biol Biotechnol. 2019; 6:21.
13. Li J, Zhang Y, Li J, Sun T, Tian C. Metabolic engineering of the cellulolytic thermophilic fungus Myceliophthora thermophila to produce ethanol from cellobiose. Biotechnol Biofuels. 2020; 13:23.
14. Liu Q, Zhang Y, Li F, Li J, Sun W, Tian C. Upgrading of efficient and scalable CRISPR-Cas-mediated technology for genetic engineering in thermophilic fungus Myceliophthora thermophila. Biotechnol Biofuels. 2019; 12:293.
15. Karnaouri A, Topakas E, Antonopoulou I, Christakopoulos P. Genomic insights into the fungal lignocellulolytic system of Myceliophthora thermophila. Front Microbiol. 2014; 5:281.
16. Kolbusz MA, Di Falco M, Ishmael N, Marqueteau S, Moisan MC, Baptista CDS, Powlowski J, Tsang A. Transcriptome and exoproteome analysis of utilization of plant-derived biomass by Myceliophthora thermophila. Fungal Genet Biol. 2014; 72:10-20.
17. Lai Y, Wang J, Xie N, Liu G, Lacap-Bugler DC. Identification of a novel forkhead transcription factor MtFKH1 for cellulase and xylanase gene expression in Myceliophthora thermophila (ATCC 42464). Microbiol Res. 2025; 294:128097.
18. Benocci T, Aguilar-Pontes MV, Zhou M, Seiboth B, de Vries RP. Regulators of plant biomass degradation in ascomycetous fungi. Biotechnol Biofuels. 2017; 10:152.
19. Huberman LB, Liu J, Qin L, Glass NL. Regulation of the lignocellulolytic response in filamentous fungi. Fungal Biology Reviews. 2016; 30:101-111.
20. Wang J, Wu Y, Gong Y, Yu S, Liu G. Enhancing xylanase production in the thermophilic fungus Myceliophthora thermophila by homologous overexpression of Mtxyr1. J Ind Microbiol Biotechnol. 2015; 42:1233-1241.
21. Dos Santos Gomes AC, Falkoski D, Battaglia E, Peng M, Nicolau de Almeida M, Coconi Linares N, Meijnen JP, Visser J, de Vries RP. Myceliophthora thermophila Xyr1 is predominantly involved in xylan degradation and xylose catabolism. Biotechnol Biofuels. 2019; 12:220.
22. Yang F, Gong Y, Liu G, Zhao S, Wang J. Enhancing Cellulase Production in Thermophilic Fungus Myceliophthora thermophila ATCC42464 by RNA Interference of cre1 Gene Expression. J Microbiol Biotechnol. 2015; 25:1101-1107.
23. Liu Q, Li J, Gao R, Li J, Ma G, Tian C. CLR-4, a novel conserved transcription factor for cellulase gene expression in ascomycete fungi. Mol Microbiol. 2019; 111:373-394.

24. Li N, Liu Y, Liu D, Liu D, Zhang C, Lin L, Zhu Z, Li H, Dai Y, Wang X, Liu Q, Tian C. MtTRC-1, a Novel Transcription Factor, Regulates Cellulase Production via Directly Modulating the Genes Expression of the Mthac-1 and Mtcbh-1 in Myceliophthora thermophila. Appl Environ Microbiol. 2022; 88:e0126322.
25. Xue F, Zhao Z, Gu S, Chen M, Xu J, Luo X, Li J, Tian C. The transcriptional factor Clr-5 is involved in cellulose degradation through regulation of amino acid metabolism in Neurospora crassa. BMC Biotechnol. 2023; 23:50.
26. Coradetti ST, Craig JP, Xiong Y, Shock T, Tian C, Glass NL. Conserved and essential transcription factors for cellulase gene expression in ascomycete fungi. Proc Natl Acad Sci U S A. 2012; 109:7397-7402.
27. Raulo R, Kokolski M, Archer DB. The roles of the zinc finger transcription factors XlnR, ClrA and ClrB in the breakdown of lignocellulose by Aspergillus niger. AMB Express. 2016; 6:5.
28. Kun RS, Garrigues S, Di Falco M, Tsang A, de Vries RP. Blocking utilization of major plant biomass polysaccharides leads Aspergillus niger towards utilization of minor components. Microb Biotechnol. 2021; 14:1683-1698.
29. Kun RS, Garrigues S, Peng M, Keymanesh K, Lipzen A, Ng V, Tejomurthula S, Grigoriev IV, de Vries RP. The transcriptional activator ClrB is crucial for the degradation of soybean hulls and guar gum in Aspergillus niger. Fungal Genet Biol. 2023; 165:103781.
30. Li Z, Yao G, Wu R, Gao L, Kan Q, Liu M, Yang P, Liu G, Qin Y, Song X, et al. Synergistic and Dose-Controlled Regulation of Cellulase Gene Expression in Penicillium oxalicum. PLoS Genet. 2015; 11:e1005509.
31. Zhao S, Yan YS, He QP, Yang L, Yin X, Li CX, Mao LC, Liao LS, Huang JQ, Xie SB, et al. Comparative genomic, transcriptomic and secretomic profiling of Penicillium oxalicum HP7-1 and its cellulase and xylanase hyper-producing mutant EU2106, and identification of two novel regulatory genes of cellulase and xylanase gene expression. Biotechnol Biofuels. 2016; 9:203.
32. Ogawa M, Kobayashi T, Koyama Y. ManR, a novel Zn(II)2Cys6 transcriptional activator, controls the beta-mannan utilization system in Aspergillus oryzae. Fungal Genet Biol. 2012; 49:987-995.
33. Ogawa M, Kobayashi T, Koyama Y. ManR, a transcriptional regulator of the beta-mannan utilization system, controls the cellulose utilization system in Aspergillus oryzae. Biosci Biotechnol Biochem. 2013; 77:426-429.
34. Hakkinen M, Valkonen MJ, Westerholm-Parvinen A, Aro N, Arvas M, Vitikainen M, Penttila M, Saloheimo M, Pakula TM. Screening of candidate regulators for cellulase and hemicellulase production in Trichoderma reesei and identification of a factor essential for cellulase production. Biotechnol Biofuels. 2014; 7:14.
35. Fujii T, Inoue H, Ishikawa K. Decreased cellulase and xylanase production in the fungus Talaromyces cellulolyticus by disruption of tacA and tctA genes, encoding putative zinc finger transcriptional factors. Appl Biochem Biotechnol. 2015; 175:3218-3229.
36. Fujii T, Inoue H, Matsushika A. The Transcription Factor Gene tclB2 Regulates

Mannanolytic Enzyme Production in the Fungus Talaromyces cellulolyticus. Appl Biochem Biotechnol. 2021; 193:3163-3172.

37. Zhang C, Li N, Rao L, Li J, Liu Q, Tian C. Development of an Efficient C-to-T Base-Editing System and Its Application to Cellulase Transcription Factor Precise Engineering in Thermophilic Fungus Myceliophthora thermophila. Microbiol Spectr. 2022; 10:e0232121.
38. Craig JP, Coradetti ST, Starr TL, Glass NL. Direct target network of the Neurospora crassa plant cell wall deconstruction regulators CLR-1, CLR-2, and XLR-1. mBio. 2015; 6:e01452-01415.
39. Frommhagen M, Koetsier MJ, Westphal AH, Visser J, Hinz SW, Vincken JP, van Berkel WJ, Kabel MA, Gruppen H. Lytic polysaccharide monooxygenases from Myceliophthora thermophila C1 differ in substrate preference and reducing agent specificity. Biotechnol Biofuels. 2016; 9:186.
40. Frommhagen M, Westphal AH, Hilgers R, Koetsier MJ, Hinz SWA, Visser J, Gruppen H, van Berkel WJH, Kabel MA. Quantification of the catalytic performance of C1-cellulose-specific lytic polysaccharide monooxygenases. Appl Microbiol Biotechnol. 2018; 102:1281-1295.
41. Kadowaki MAS, Varnai A, Jameson JK, AE TL, Costa-Filho AJ, Kumagai PS, Prade RA, Polikarpov I, Eijsink VGH. Functional characterization of a lytic polysaccharide monooxygenase from the thermophilic fungus Myceliophthora thermophila. PLoS One. 2018; 13:e0202148.
42. Karnaouri A, Muraleedharan MN, Dimarogona M, Topakas E, Rova U, Sandgren M, Christakopoulos P. Recombinant expression of thermostable processive MtEG5 endoglucanase and its synergism with MtLPMO from Myceliophthora thermophila during the hydrolysis of lignocellulosic substrates. Biotechnol Biofuels. 2017; 10:126.
43. Coradetti ST, Xiong Y, Glass NL. Analysis of a conserved cellulase transcriptional regulator reveals inducer-independent production of cellulolytic enzymes in Neurospora crassa. Microbiologyopen. 2013; 2:595-609.
44. Xu G, Li J, Liu Q, Sun W, Jiang M, Tian C. Transcriptional analysis of Myceliophthora thermophila on soluble starch and role of regulator AmyR on polysaccharide degradation. Bioresour Technol. 2018; 265:558-562.
45. Cai P, Wang B, Ji J, Jiang Y, Wan L, Tian C, Ma Y. The putative cellodextrin transporter-like protein CLP1 is involved in cellulase induction in Neurospora crassa. J Biol Chem. 2015; 290:788-796.
46. Li X, Chomvong K, Yu VY, Liang JM, Lin Y, Cate JHD. Cellobionic acid utilization: from Neurospora crassa to Saccharomyces cerevisiae. Biotechnol Biofuels. 2015; 8:120.
47. Visser H, Joosten V, Punt PJ, Gusakov AV, Olson PT, Joosten R, Bartels J, Visser J, Sinitsyn AP, Emalfarb MA. Development of a mature fungal technology and production platform for industrial enzymes based on a Myceliophthora thermophila isolate, previously known as Chrysosporium lucknowense C1. Industrial Biotechnology. 2011; 7:214-223.

48. Zhu Z, Zhang M, Liu D, Liu D, Sun T, Yang Y, Dong J, Zhai H, Sun W, Liu Q, Tian C. Development of the thermophilic fungus Myceliophthora thermophila into glucoamylase hyperproduction system via the metabolic engineering using improved AsCas12a variants. Microb Cell Fact. 2023; 22:150.
49. Gu S, Zhao Z, Xue F, Liu D, Liu Q, Li J, Tian C. The arabinose transporter MtLat-1 is involved in hemicellulase repression as a pentose transceptor in Myceliophthora thermophila. Biotechnol Biofuels Bioprod. 2023; 16:51.
50. Zhao Z, Gu S, Liu D, Liu D, Chen B, Li J, Tian C. The putative methyltransferase LaeA regulates mycelium growth and cellulase production in Myceliophthora thermophila. Biotechnol Biofuels Bioprod. 2023; 16:58.
51. Li N, Kunitake E, Aoyama M, Ogawa M, Kanamaru K, Kimura M, Koyama Y, Kobayashi T. McmA-dependent and -independent regulatory systems governing expression of ClrB-regulated cellulase and hemicellulase genes in Aspergillus nidulans. Mol Microbiol. 2016; 102:810-826.
52. Petibon C, Malik Ghulam M, Catala M, Abou Elela S. Regulation of ribosomal protein genes: An ordered anarchy. Wiley Interdiscip Rev RNA. 2021; 12:e1632.
53. Hogues H, Lavoie H, Sellam A, Mangos M, Roemer T, Purisima E, Nantel A, Whiteway M. Transcription factor substitution during the evolution of fungal ribosome regulation. Mol Cell. 2008; 29:552-562.
54. Shore D, Zencir S, Albert B. Transcriptional control of ribosome biogenesis in yeast: links to growth and stress signals. Biochem Soc Trans. 2021; 49:1589-1599.
55. Powers T, Walter P. Regulation of ribosome biogenesis by the rapamycin-sensitive TOR-signaling pathway in Saccharomyces cerevisiae. Mol Biol Cell. 1999; 10:987-1000.
56. Marion RM, Regev A, Segal E, Barash Y, Koller D, Friedman N, O'Shea EK. Sfp1 is a stress- and nutrient-sensitive regulator of ribosomal protein gene expression. Proc Natl Acad Sci U S A. 2004; 101:14315-14322.
57. Lempiainen H, Uotila A, Urban J, Dohnal I, Ammerer G, Loewith R, Shore D. Sfp1 interaction with TORC1 and Mrs6 reveals feedback regulation on TOR signaling. Mol Cell. 2009; 33:704-716.
58. Tian C, Kasuga T, Sachs MS, Glass NL. Transcriptional profiling of cross pathway control in Neurospora crassa and comparative analysis of the Gcn4 and CPC1 regulons. Eukaryot Cell. 2007; 6:1018-1029.
59. Griffioen G, Mager WH, Planta RJ. Nutritional upshift response of ribosomal protein gene transcription in Saccharomyces cerevisiae. FEMS Microbiol Lett. 1994; 123:137-144.
60. Griffioen G, Laan RJ, Mager WH, Planta RJ. Ribosomal protein gene transcription in Saccharomyces cerevisiae shows a biphasic response to nutritional changes. Microbiology (Reading). 1996; 142 (Pt 8):2279-2287.
61. Shi YG, Tyler BM. Coordinate expression of ribosomal protein genes in Neurospora crassa and identification of conserved upstream sequences. Nucleic Acids Res. 1991; 19:6511-6517.
62. Natarajan K, Meyer MR, Jackson BM, Slade D, Roberts C, Hinnebusch AG,

Marton MJ. Transcriptional profiling shows that Gcn4p is a master regulator of gene expression during amino acid starvation in yeast. Mol Cell Biol. 2001; 21:4347-4368.

63. Xie S, Shen B, Zhang C, Huang X, Zhang Y. sgRNAcas9: a software package for designing CRISPR sgRNA and evaluating potential off-target cleavage sites. PLoS One. 2014; 9:e100448.
64. Li Y, Yan P, Lu X, Qiu Y, Liang S, Liu G, Li S, Mou L, Xie N. Involvement of PaSNF1 in Fungal Development, Sterigmatocystin Biosynthesis, and Lignocellulosic Degradation in the Filamentous Fungus Podospora anserina. Front Microbiol. 2020; 11:1038.
65. Livak KJ, Schmittgen TD. Analysis of relative gene expression data using real-time quantitative PCR and the 2(-Delta Delta C(T)) Method. Methods. 2001; 25:402-408.
66. Kim D, Langmead B, Salzberg SL. HISAT: a fast spliced aligner with low memory requirements. Nat Methods. 2015; 12:357-360.
67. Li B, Dewey CN. RSEM: accurate transcript quantification from RNA-Seq data with or without a reference genome. BMC Bioinformatics. 2011; 12:323.
68. Love MI, Huber W, Anders S. Moderated estimation of fold change and dispersion for RNA-seq data with DESeq2. Genome Biol. 2014; 15:550.

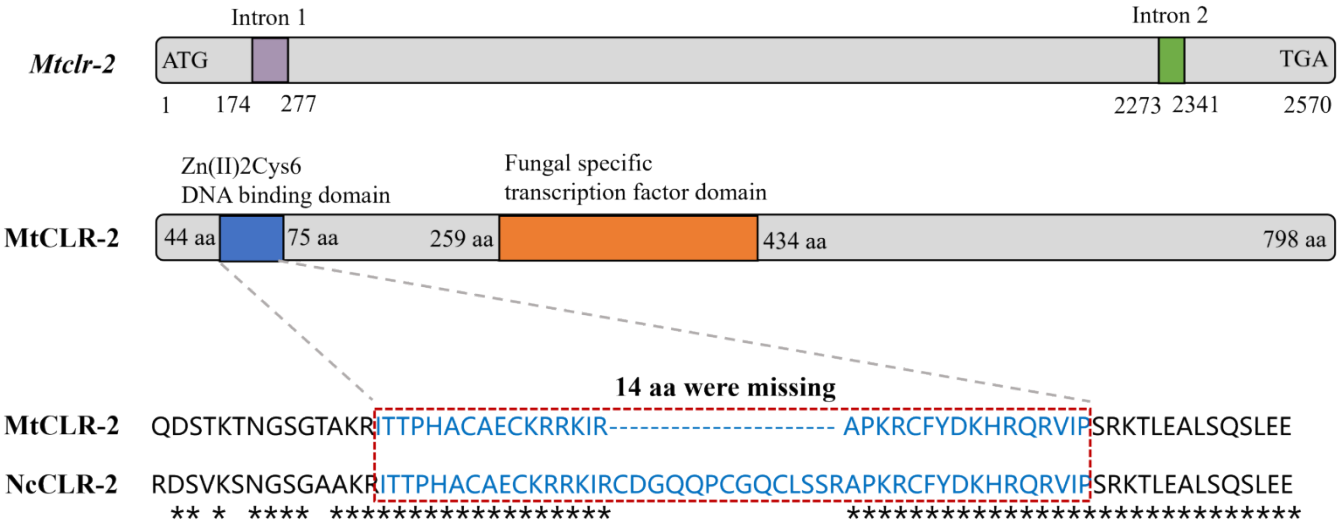

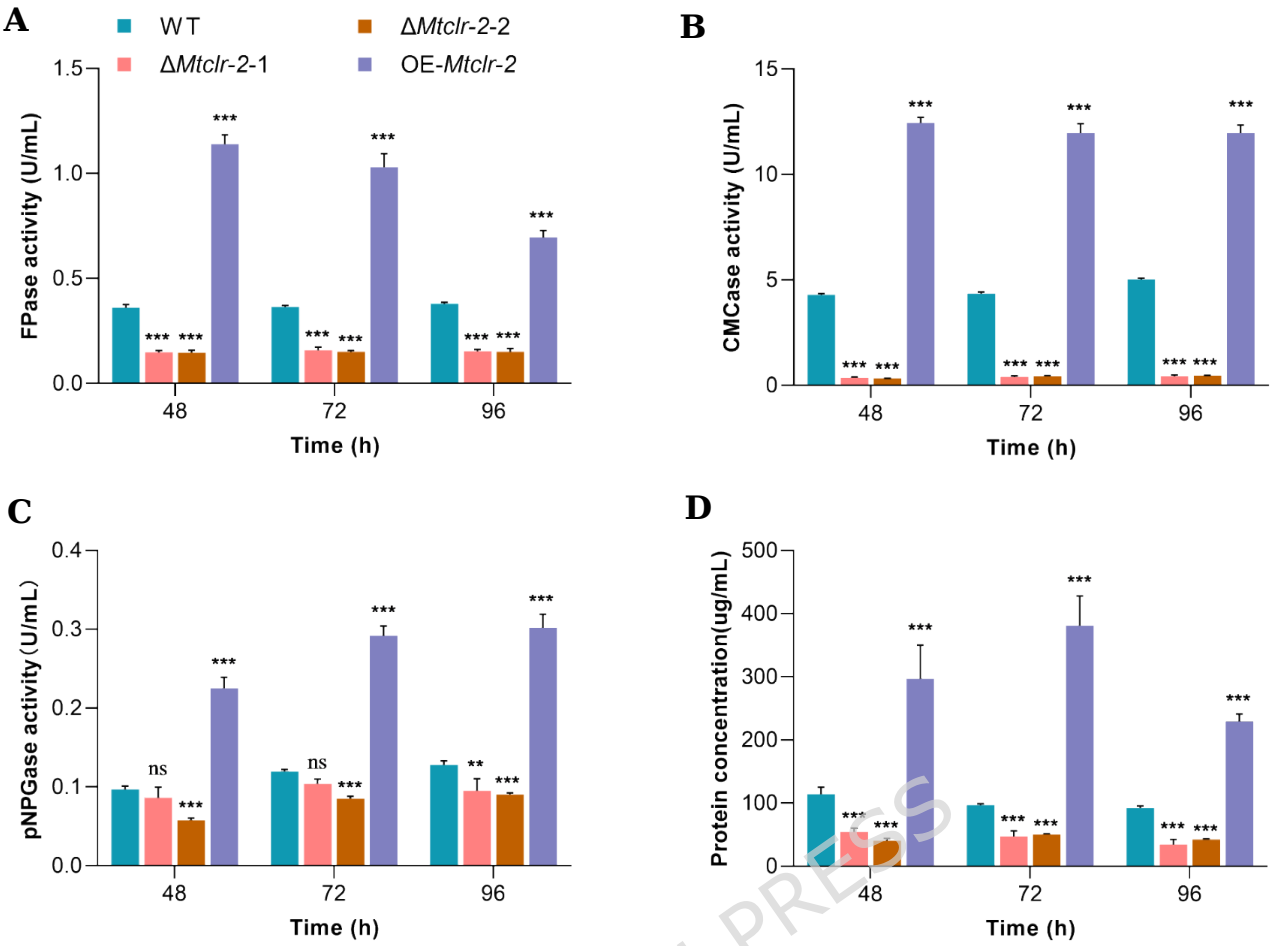

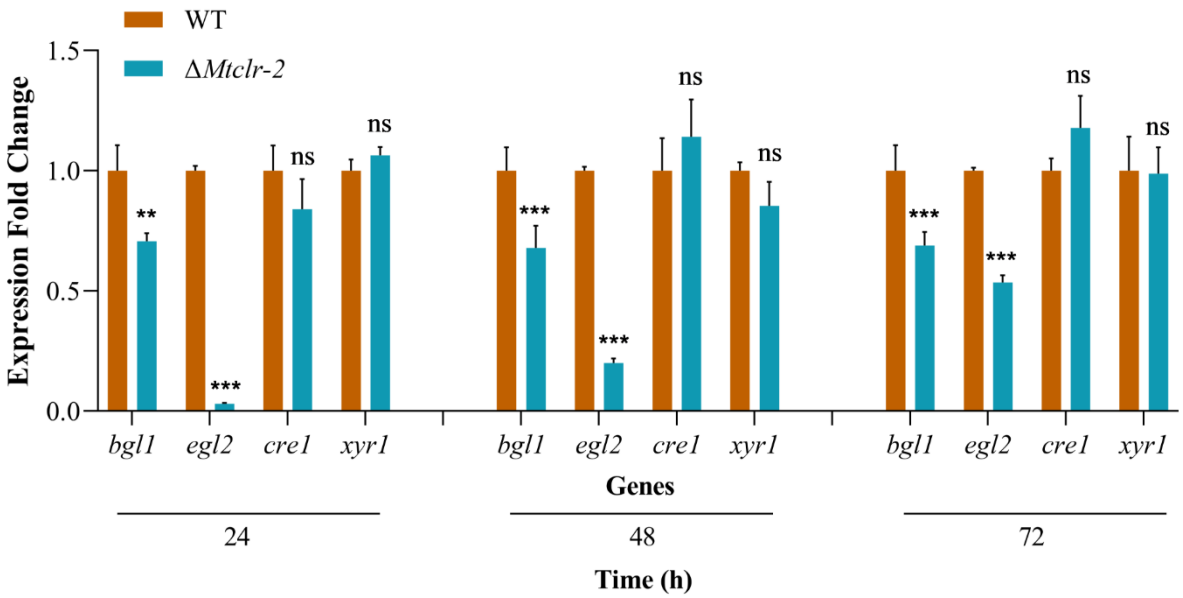

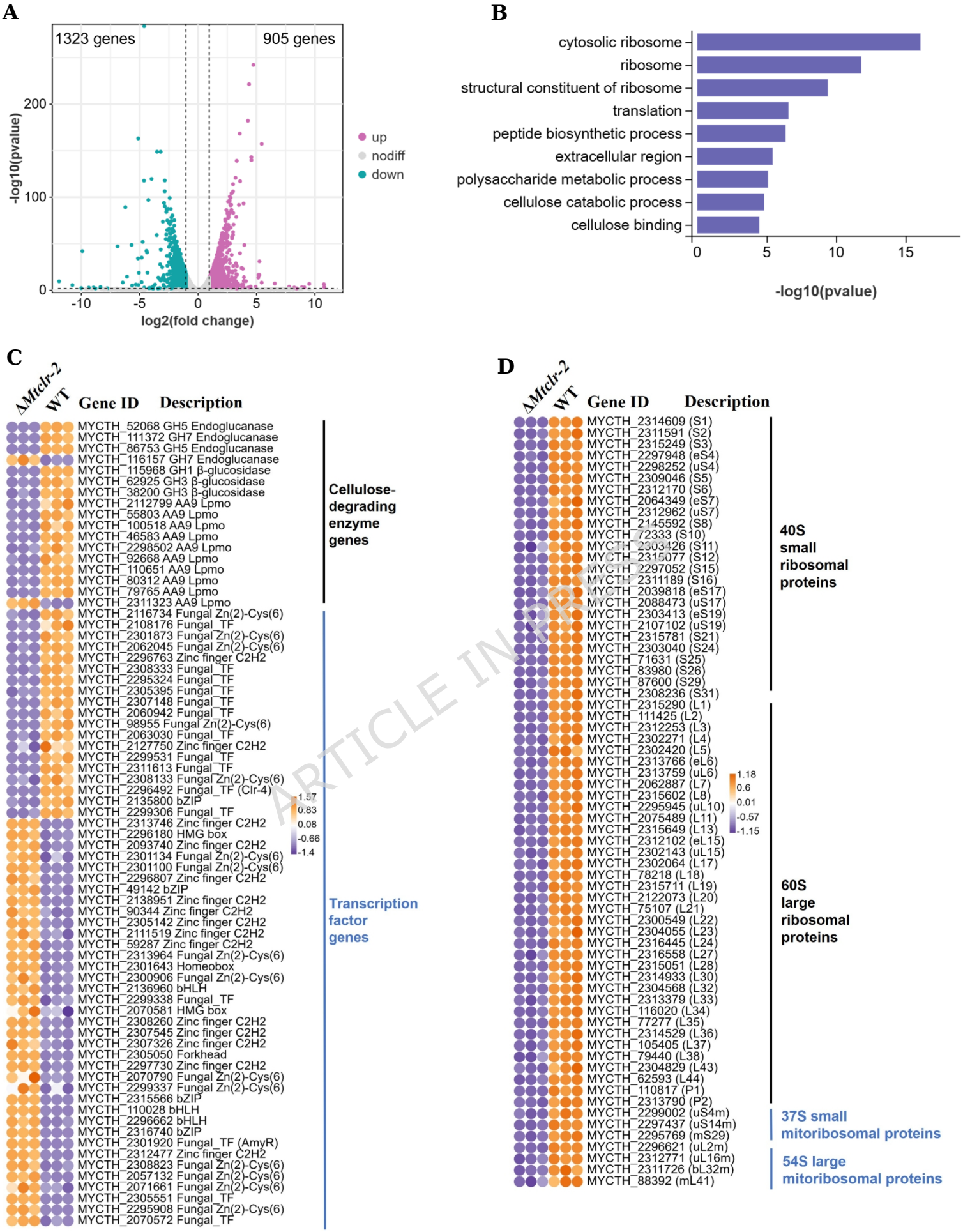

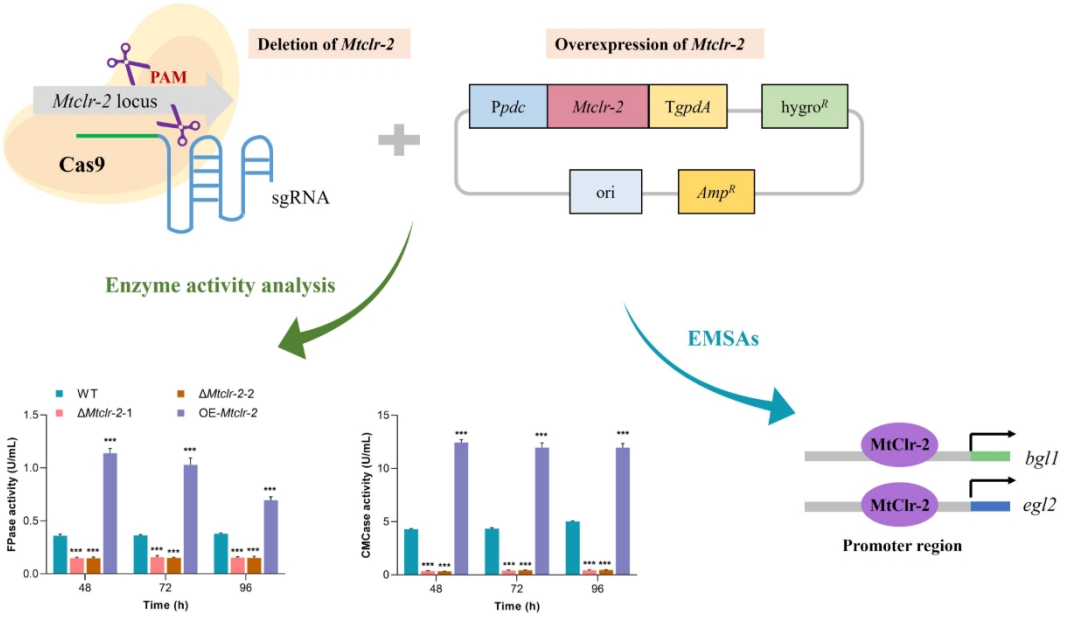

Through a combination of gene deletion, overexpression analyses, and electrophoretic mobility shift assays, we demonstrate that MtClr-2 functions as an activator of cellulase production by directly regulating the expression of the major cellulase genes *egl2* and *bgl1* through promoter binding.

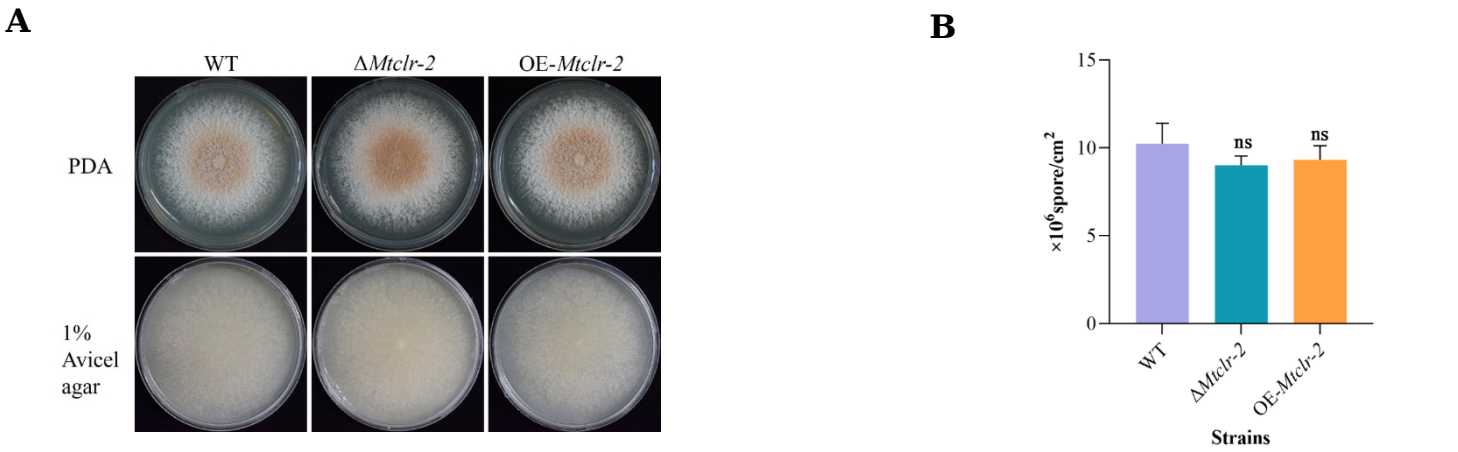

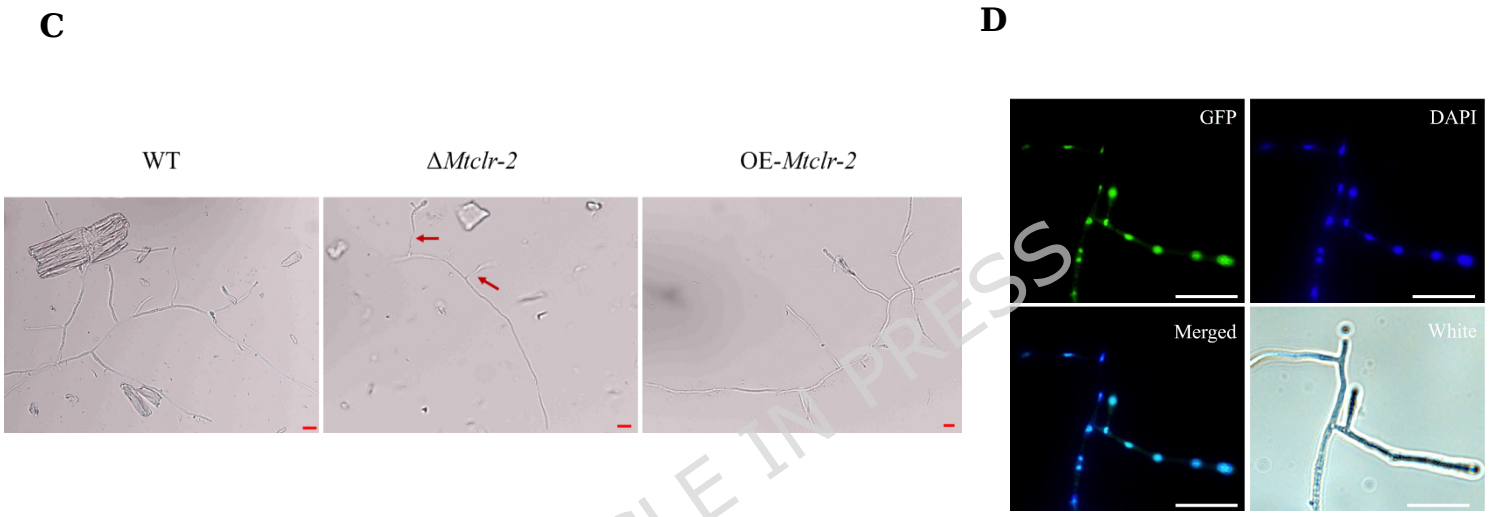

A

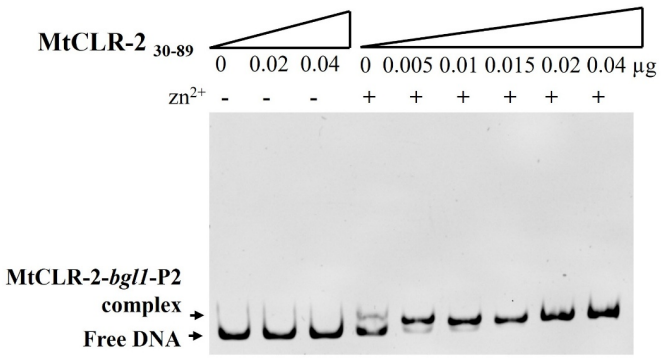

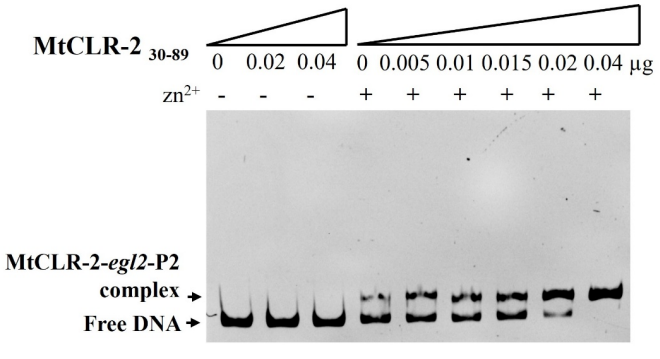

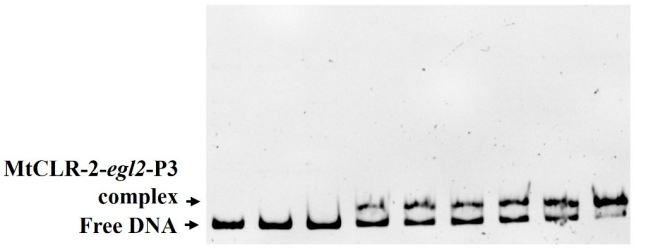

B

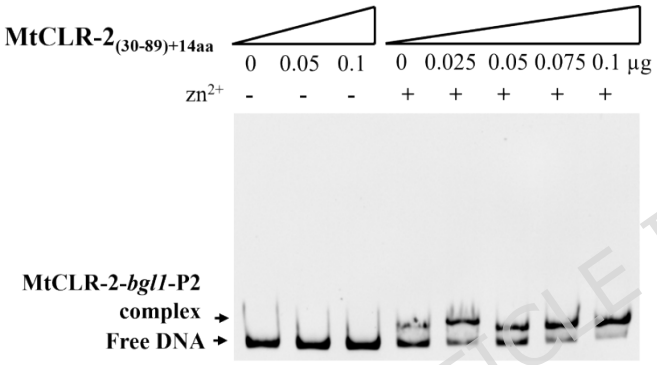

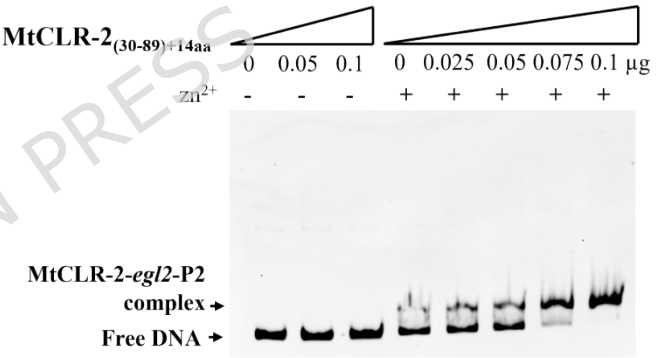

C